Heliyon 10 (2024) e24668

Contents lists available at ScienceDirect

Heliyon

journal homepage: www.cell.com/heliyon

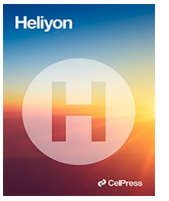

Research article

Long noncoding RNA lnc-SNAPC5-3:4 inhibits malignancy by directly upregulating miR-224-3p in non-small cell lung cancer

Chenxi Hu [a,1], Shuo Wu [b,1], Wen Sun [a], Jiawen Li [c], Kaiyuan Hui [a,**], Xiaodong Jiang [a,b,*]

[a] Department of Oncology, The Affiliated Lianyungang Hospital of Xuzhou Medical University, Lianyungang, 222061, Jiangsu, China
[b] Department of Oncology, Lianyungang Clinical College of Nanjing Medical University, Lianyungang, 222061, Jiangsu, China
[c] Department of Pharmacy, The Affiliated Lianyungang Hospital of Xuzhou Medical University, Lianyungang, 222061, Jiangsu, China

ARTICLE INFO

Keywords:
Non-small cell lung cancer
lnc-SNAPC5-34
miR-224-3p

ABSTRACT

The mounting body of evidence demonstrates the growing importance of long noncoding RNAs in the advancement of tumors. This study aimed to investigate the molecular mechanism of lnc-SNAPC5-3:4 in non-small cell lung cancer (NSCLC). We investigated the expression of miR-224-3p and lnc-SNAPC5-3:4 in clinical NSCLC samples and NSCLC cell lines using reverse transcription polymerase chain reaction (RT-PCR). *In vitro* studies, A549 cell growth was estimated using Cell Counting Kit-8 (CCK-8), 5-ethynyl-2′-deoxyuridine (EDU), and flow cytometry assays. *In vivo* studies, NSCLC tumorigenesis was determined using xenograft tumor mouse models, tumor growth was evaluated using antigen Kiel 67 (Ki67) staining, and tumor apoptosis was detected through terminal deoxynucleotidyl transferase dUTP nick end labeling (TUNEL) staining. The relationship between lnc-SNAPC5-3:4 and miR-224-3p was determined by luciferase reporter gene assay. Results indicated that the expression of lnc-SNAPC5-3:4 was observed to be downregulated in NSCLC tissues and cell lines. After overexpression of lnc-SNAPC5-3:4 in cultured A549 cells, proliferation decreased and apoptosis increased. Furthermore, the expression of miR-224-3p was targeted and negatively regulated by lnc-SNAPC5-3:4. The lnc-SNAPC5-3:4 upregulation inhibited cell proliferation and promoted apoptosis, which was partially blocked by miR-224-3p overexpression in A549 cells. In addition, we constructed a subcutaneous inoculation model using BALB/c nude mice, and the results indicated that lnc-SNAPC5-3:4 overexpression restrained the growth of subcutaneous tumors, decreased Ki67 expression levels, and increased apoptosis, as indicated by TUNEL staining in nude mice. However, miR-224-3p transfection resulted in the reversal of the inhibitory effect of lnc-SNAPC5-3:4 on tumor growth. In conclusion, our study revealed that lnc-SNAPC5-3:4 inhibits tumor progression in NSCLC by targeting miR-224-3p. This study provides a potential therapeutic target for inhibiting NSCLC progression.

* Corresponding author. Department of Oncology, The Affiliated Lianyungang Hospital of Xuzhou Medical University, Lianyungang, 222061, Jiangsu, China.
** Corresponding author. Department of Oncology, The Affiliated Lianyungang Hospital of Xuzhou Medical University, Lianyungang, 222061, Jiangsu, China.
E-mail addresses: kyhui1987@163.com (K. Hui), jxdpaper@163.com (X. Jiang).
[1] These authors were contributed equally.

https://doi.org/10.1016/j.heliyon.2024.e24668
Received 7 November 2023; Received in revised form 24 December 2023; Accepted 11 January 2024
Available online 13 January 2024

1. Introduction

Lung cancer is a highly prevalent and deadly malignancy of the bronchial mucosa or glands of the lungs [1]. Non-small cell lung cancer (NSCLC) is the most prevalent type, comprising approximately 80 % of all cases [2]. Unfortunately, owing to the nonspecific early symptoms of this disease, the prognosis is often unfavorable because the 5-year survival rate is typically below 20 % [3]. Therefore, it is essential to conduct more research to explore the pathogenesis of lung cancer, find biomarkers for early diagnosis, and develop new treatment strategies.

Long non-coding RNAs (lncRNAs) play an important role in various biological processes in lung cancer cells [4]. Studies have shown the ability of lnc-THOR to promote NSCLC cell growth by binding to IGF2BP1 at the *in vitro* level. *In vivo*, intratumoral injection of lnc-THOR shRNA adeno-associated virus effectively inhibited the tumor growth of A549 xenograft in nude mice [5]. The expression level of lncRNAs SOX21-AS1 is high in lung cancer tissues and cells. However, the expression level of miR-24-3p bound to lncRNAs SOX21-AS1 was relatively low. Knockdown of SOX21-AS1 reduced cell proliferation, activated apoptosis, and promoted cell migration and invasion. These effects were abolished by miR-24-3p inhibition [6]. Lnc-SNAPC5-3:4 expression was significantly upregulated when anlotinib treatment was effective and downregulated when anlotinib treatment failed in NSCLC [7]. This finding suggests that lnc-SNAPC5-3:4 may affect the therapeutic mechanism of anlotinib and that its expression level could be used as an indicator of treatment response. Additional research is necessary to elucidate the specific mechanisms through which lnc-SNAPC5-3:4 operates in the treatment of non-small cell lung cancer (NSCLC), providing valuable insights for the advancement of personalized therapeutic strategies.

Many malignancies, autoimmune conditions, and neurological illnesses develop and advance due to the presence of microRNAs (miRNAs). MiR-4757-3p is down-regulated in A549 cells, and miR-4757-3p inhibits the migration and invasion of lung cancer cells by inhibiting the activation of the Wnt signaling pathway [8]. In addition, abnormal upregulation of miR-224-3p expression has been observed in various malignant tumors [9–12], including NSCLC, where it promotes cell proliferation and inhibits apoptosis [13]. DHRS4-AS1 partially reversed miR-224-3p-reduced TP53 and TET1, thereby suppressing tumor growth *in vivo* [14]. Studies have shown that miR-224 is significantly up-regulated in NSCLC tissues and positively correlated with the occurrence and metastasis of NSCLC. *In vitro* experiments showed that miRNA-224 promoted the proliferation and invasion of A549 cells, and inhibited cell apoptosis [15]. Taken together, it is reasonable to hypothesize that the interaction between lnc-SNAPC5-3:4 and miR-224-3p exists and may play an important regulatory role in NSCLC progression.

We hypothesized that lnc-SNAPC5-3:4 could inhibit the proliferation, migration, and invasion of NSCLC cells and promote cell apoptosis by binding to miR-224-3p. The main aim of the present study was to elucidate this regulatory relationship from the *in vitro* and *in vivo* levels.

2. Materials and methods

2.1. Cell culture

Three human lung cancer cell lines (NCI–H1299, A549, and SPC-A1) and one normal human lung epithelial cell line (16HBE) were obtained from the Cell Bank of the Chinese Academy of Sciences. NCI–H1299, 16HBE and SPC-A1 were cultured in RPMI-1640 (Gibco, cat#11875093), A549 was cultured in Ham's F–12K (Gibco, cat#21127022) with 10 % fetal bovine serum (Gibco, cat#10099) and 0.5 % penicillin/streptomycin (Gibco, cat#15640055), and maintained at 37 °C in a 5 % CO_2 incubator.

2.2. Cell transfection

A549 cells (1×10^5 cells/pores) were inoculated in a 6-well culture plate containing a complete medium 24 h before transfection. NC mimics (50 nM) or miR-224-3p mimics (50 nM) or pcDNA3.1 vector (8 μg) or pcDNA3.1-Snapc5-3:4 (8 μg) were treated with Lipofectamine 2000 (Invitrogen; Thermo Fisher Technologies) into A549 cells. 24 h after transfection, the cells were treated and harvested.

2.3. Clinical samples

Clinical tissues (NSCLC and adjacent normal tissues) were freshly collected from five patients following the appropriate ethical guidelines. Written consent forms were signed by the participants to ensure their understanding and agreement to participate in the study. The inclusion criteria were as follows: NSCLC was verified through pathology, cytology, and imaging examination; no history of radiotherapy, chemotherapy, or surgical intervention before admission; specimens were preserved; and follow-up data were complete. The exclusion criteria were as follows: immune system disease; small cell lung cancer or other malignant tumors; and severe cardiac, liver, and renal insufficiency.

2.4. Reverse transcription-polymerase chain reaction (PCR)

TRIzol was used to isolate and purify total RNA from cells or tissues. RNA (1 μg) was added for reverse transcription, and complementary DNA (cDNA) was obtained by Avian Myeloblastosis Virus RT. Subsequently, the RT-quantitative PCR (qPCR) reaction system was formulated by mixing cDNA, specific primers, and TB Green® Premix Ex Taq™ II FAST qPCR (Takara, Japan). The PCR

amplification protocol involved 3 min denaturation at 95 °C, followed by 40 repetitive cycles (15 s at 95 °C and 45 s at 60 °C). Gene expression ploidy changes relative to the internal reference glyceraldehyde 3-phosphate dehydrogenase (GAPDH) were used as the internal reference gene to normalize the expression of other target genes. Gene expression was calculated using the $2^{-\Delta\Delta Ct}$ formula, and the results after three biological replicates were counted. The primer sequences used were as follows: lnc-SNAPC5-3:4 (Forward: TCAAGATGTTGGTGCATGT, Reverse: AGCCATTTTTGCAACTACAC); miR-224-3p (Forward: TGATGTGGGTGCTGGTGTC, Reverse: TTGTGTTGGGGCAGTACTG); and GAPDH (Forward: AGAAGGCTGGGGCTCATTTG, Reverse: AGGGGCCATCCACAGTCTTC).

2.5. Cell Counting Kit-8 (CCK-8) assay

Cell viability was determined using a CCK-8 kit (Abcam, cat#ab228554). Cells were seeded in 96-well plates at a density of 1×10^4 cells/well. The optical density was measured every 24 h. CCK-8 solution and medium were added to the cells in the ratio of 1:10, and the cells were incubated at 37 °C for 1 h to detect using a microplate reader.

2.6. 5-ethynyl-2′-deoxyuridine (EdU) assay

In order to assess the proliferative capacity of A549 cells, an EdU assay was conducted. EdU assays of A549 cells were performed using an EdU Staining Proliferation Kit. The cells were cultured in EdU solution for 2–4 h, the fixing solution was added, and then the cells were incubated for 15 min. Permeabilization buffer was added and the mixture was incubated for 15 min. The reaction mixture was fluorescently labeled with EdU and incubated for 30 min. Cells were observed and photographed using a fluorescence microscope.

2.7. Flow cytometry

An apoptosis analysis kit was used to analyze apoptosis. Briefly, A549 cells were seeded in six-well plates and collected. The cells were then fixed with cool alcohol for 1 h and filtered through 400-mesh strainers to obtain a single-cell suspension. After treatment, cells were collected and the concentration was adjusted to 1×10^6 cells/mL, and then mixed with 5 μl of Annexin V or PI, left in a dimly lit room for 20 min. Finally, the apoptosis rate of the cells was analyzed using flow cytometry (BD FACSAria III, US).

2.8. Western blotting

To examine protein expression levels, Western blotting experiments were performed. Proteins were extracted from tissues and cells using a radioimmunoprecipitation assay buffer (Thermo Fisher Scientific) and quantified using a bicinchoninic acid kit. The protein samples of each group were loaded with 30 μg and then transferred to polyvinylidene fluoride membranes (Thermo Fisher Scientific). The membranes were blocked with 5 % skim milk and incubated with antibodies against Bax (CST#2774; 1:1000), actin (CST#4967; 1:1000), and Caspase3 (CST#9662; 1:1000) overnight at 4 °C. Subsequently, the membranes were incubated with Goat Anti-Rabbit IgG H&L (horseradish peroxidase) secondary antibodies (cat#ab6721; 1:1000) for 2 h, washed with phosphate-buffered saline with Tween® 20 three times, and incubated in the dark. Protein bands were visualized using chemiluminescence and ImageJ software to examine the grayscale values.

2.9. Double luciferase reporter gene assay

One day before transfection, 293T cells were seeded into a 48-well culture plate. A transfection reagent (1 μL) and a 0.2 μg plasmid were diluted in 30 μL of the culture medium. The mixture was then incubated at room temperature for 20 min. Following the removal of the culture medium from the wells, each well of the 48-well culture plate was supplemented with 50 μL of the transfection mixture and incubated at 37 °C for 5 h. After removing the liquid, 0.2 mL of fresh culture medium was added to each well, and the plate was subsequently incubated at 37 °C for an additional 48 h. Following the incubation period, 200 μL of cell lysis buffer was introduced to each well and allowed to incubate at room temperature for 10 min. The lysates were collected and 20 μL of the supernatant was transferred to a 96-well fluorescence plate. Subsequently, 100 μL of luciferase detection reagent was added. After thorough mixing, the luminescence intensity was measured, and 100 μL of Stop & Glo® Reagent was added to the samples. The luminescence was measured again after mixing.

2.10. Animal model

Female nude mice (4–6 weeks old) were purchased from Vital River. Mice were randomly divided into four groups: pc-NC (lnc-SNAPC5-3:4 overexpression negative control); pc-SNAPC5-34 (lnc-SNAPC5-3:4 overexpression); pc-SNAPC5-34 + NC mimic (lnc-SNAPC5-3:4 overexpression co-transfected with miR-224-3p mimic negative control); and pc-SNAPC5-34 + miR-224-3p mimic (lnc-SNAPC5-3:4 overexpression co-transfected with miR-224-3p mimic). The concentration of A549 cells was adjusted to 5×10^7 cells/mL with PBS, and 100 μL of cells were inoculated into the subcutaneous tissue of the right abdomen for each nude mouse. The length, width, and thickness of the tumors were measured using calipers every three days. Thirty days after injection, the experimental mice bearing xenograft tumors were euthanized, and the tumors were removed and weighed. The tumor volume was calculated as 1/2 × long diameter × short diameter2.

2.11. Immunohistochemistry (IHC)

Paraffin sections of tumor tissue were dewaxed and incubated with 3 % H_2O_2 to block endogenous peroxidase activity. The closed sections were incubated overnight with anti-Kiel 67 (Ki67) (ab15580, 1:1000, Abcam) antibodies at 4 °C and then sequentially incubated with biotin-labeled secondary antibodies. The sections were then stained with 3,3′-diaminobenzidine. Finally, the sections were stained with hematoxylin and fixed.

2.12. Terminal deoxynucleotidyl transferase dUTP nick end labeling (TUNEL) staining

Tumor tissue sections embedded in paraffin were deparaffinized and incubated with proteinase K for 30 min at 37 °C. The sections were incubated with fresh TUNEL reaction solution for 1 h at 37 °C according to the manufacturer's instructions. After staining with DAB solution for 10 min at 25 °C, sections were counterstained with hematoxylin for 10 s. Finally, TUNEL-positive cells were counted under a microscope (Olympus, Tokyo, Japan).

2.13. Statistical analysis

All statistics were acquired after at least three independent repeats and data are presented as mean ± standard error. Differences between two groups were compared using Student's t-test, and comparisons between three or more groups were performed using one-way ANOVA followed by Tukey's post hoc analysis. Data analysis using GraphPad Prism 6.0 software. Differences were considered statistically significant at $p < 0.05$.

3. Results

3.1. Expression of lnc-SNAPC5-3:4 in NSCLC

To investigate the contribution of lnc-SNAPC5-3:4 to NSCLC, it was essential to determine its expression patterns. Thus, we examined the expression pattern of lnc-SNAPC5-3:4 in tumor tissues from patients with NSCLC and compared them with that in adjacent paracancerous tissues. Significant downregulation of lnc-SNAPC5-3:4 expression in tumor tissues relative to paracancerous tissues was observed (Fig. 1A). This suggests that decreased lnc-SNAPC5-3:4 may contribute to the initiation and progression of NSCLC. To identify an appropriate cellular model for further investigation, we compared the expression levels of lnc-SNAPC5-3:4 in several NSCLC cell lines (A549, SPC-A1, and H1299) with those in normal human lung epithelial cells (16HBE). Notably, lnc-SNAPC5-3:4 expression in 16HBE cells was markedly higher than that in the three tumor cell lines, with A549 demonstrating the lowest expression level (Fig. 1B).

3.2. Up-regulation of lnc-SNAPC5-3:4 inhibits proliferation of NSCLC cells and promotes apoptosis

Based on the lnc-SNAPC5-3:4 expression pattern in different cells, we selected A549 cells as the primary research model to investigate the effect of lnc-SNAPC5-3:4 on the proliferation and apoptosis of NSCLC cells. Given that low lnc-SNAPC5-3:4 expression may contribute to NSCLC progression, we initially established an lnc-SNAPC5-3:4-overexpressing A549 cell line using RT-PCR-based transfection (Fig. 2A). Subsequently, CCK-8 and EdU assays revealed reduced activity and proliferative capacity in A549 cells overexpressing lnc-SNAPC5-3:4, whereas Annexin V-FITC/PI detection indicated an elevated level of apoptosis (Fig. 2B–D). Furthermore, Western blot analysis demonstrated the upregulation of apoptosis-related proteins (Bax and Caspase 3) in A549 cells overexpressing lnc-SNAPC5-3:4 (Fig. 2E). Collectively, these findings suggest that lnc-SNAPC5-3:4 impedes proliferation and promotes apoptosis of A549 cells and that the decrease in lnc-SNAPC5-3:4 during tumor progression is one of the contributing factors to spatial and temporal

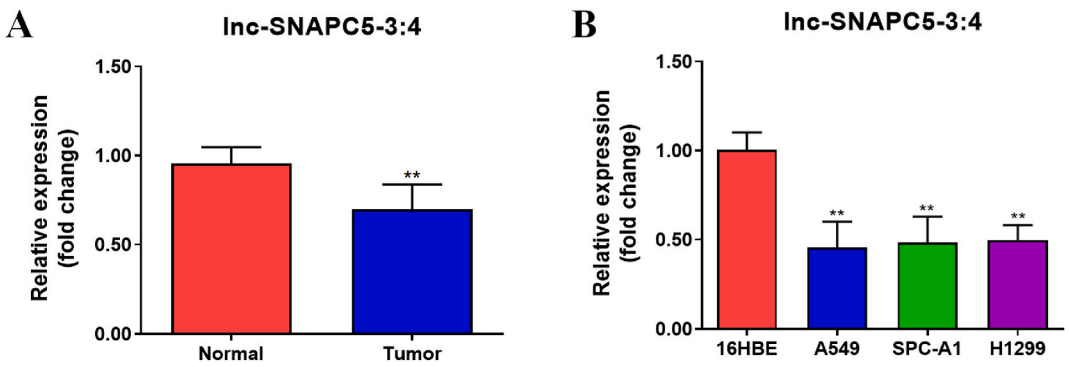

Fig. 1. Expression of lnc-SNAPC5-3:4 in non-small cell lung cancer (NSCLC) cells A. Expression of lnc-SNAPC5-3:4 in NSCLC (n = 5) and paracancerous tissues (n = 5). B. Expression of lnc-SNAPC5-3:4 in NSCLC cell lines. Data are shown as mean ± SD, **P < 0.01.

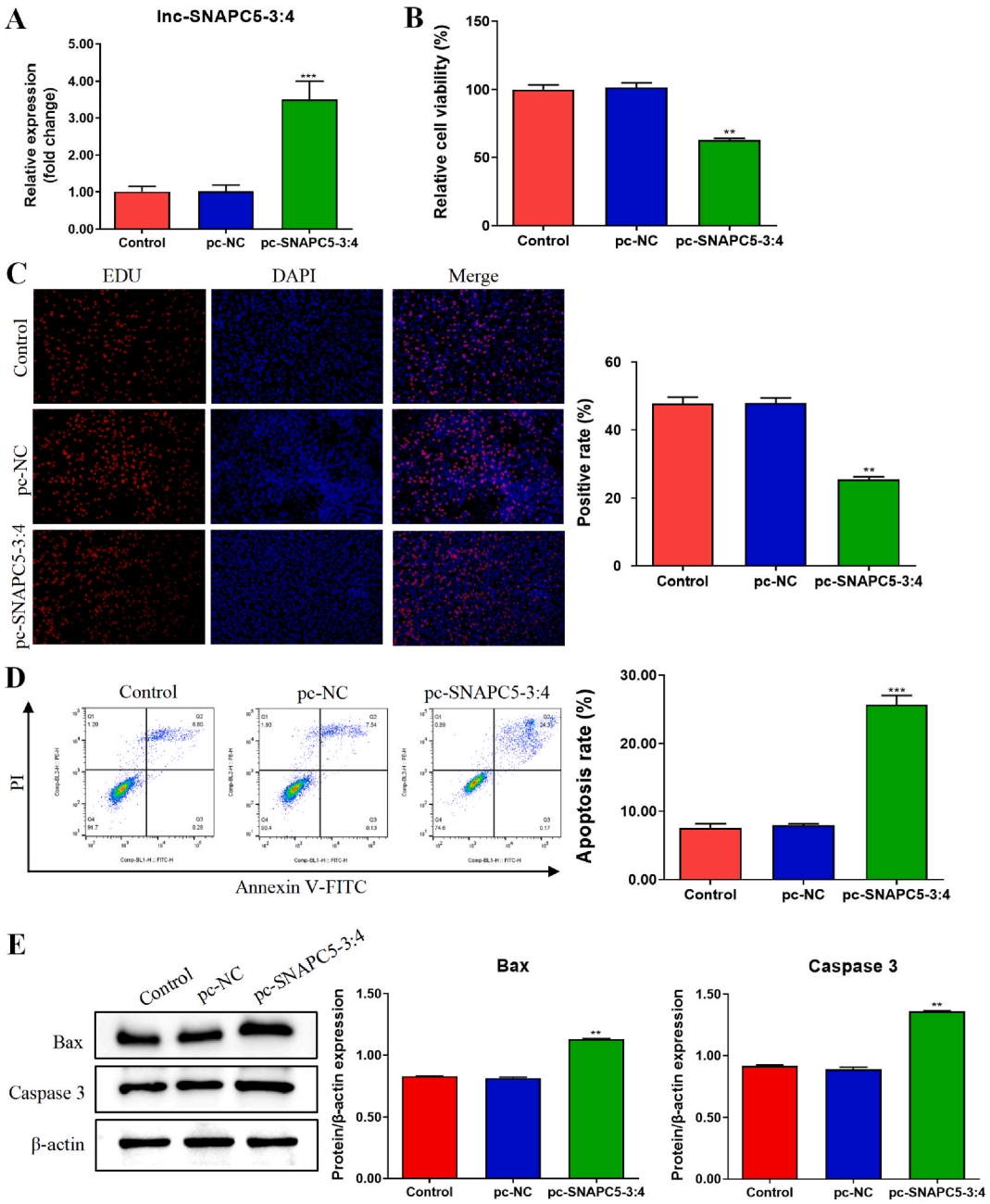

Fig. 2. Upregulation of lnc-SNAPC5-3:4 inhibited the proliferation of non-small cell lung cancer (NSCLC) cells and promoted apoptosis. Efficiency of lnc-SNAPC5-3:4 overexpression in A549 cells. B. The activity of A549 cells was determined using a Cell Counting Kit-8 (CCK-8) assay. C. The proliferation of A549 cells was detected using the 5-ethynyl-2′-deoxyuridine (EdU) assay. D. The apoptosis of A549 cells was detected using fluorescence-activated cell sorting (FACS). E. The expression levels of Bax and Caspase3 in A549 cells were determined using western blotting. Data are shown as mean ± SD, **P < 0.01, ***P < 0.001.

tumor growth.

3.3. The regulation between lnc-SNAPC5-3:4 and miR-224-3p

As previously mentioned, lnc-SNAPC5-3:4 inhibits A549 cell proliferation and promotes apoptosis, although the specific mechanism of action remains unclear. To investigate the molecular mechanism of lnc-SNAPC5-3:4, we used the lncRNASNP2 database to predict potential target interactions involving lnc-SNAPC5-3:4. We identified a binding site between lnc-SNAPC5-3:4 and miR-224-3p (Fig. 3A). In addition, we evaluated the expression profile of miR-224-3p in NSCLC cells. In contrast to lnc-SNAPC5-3:4, miR-224-3p

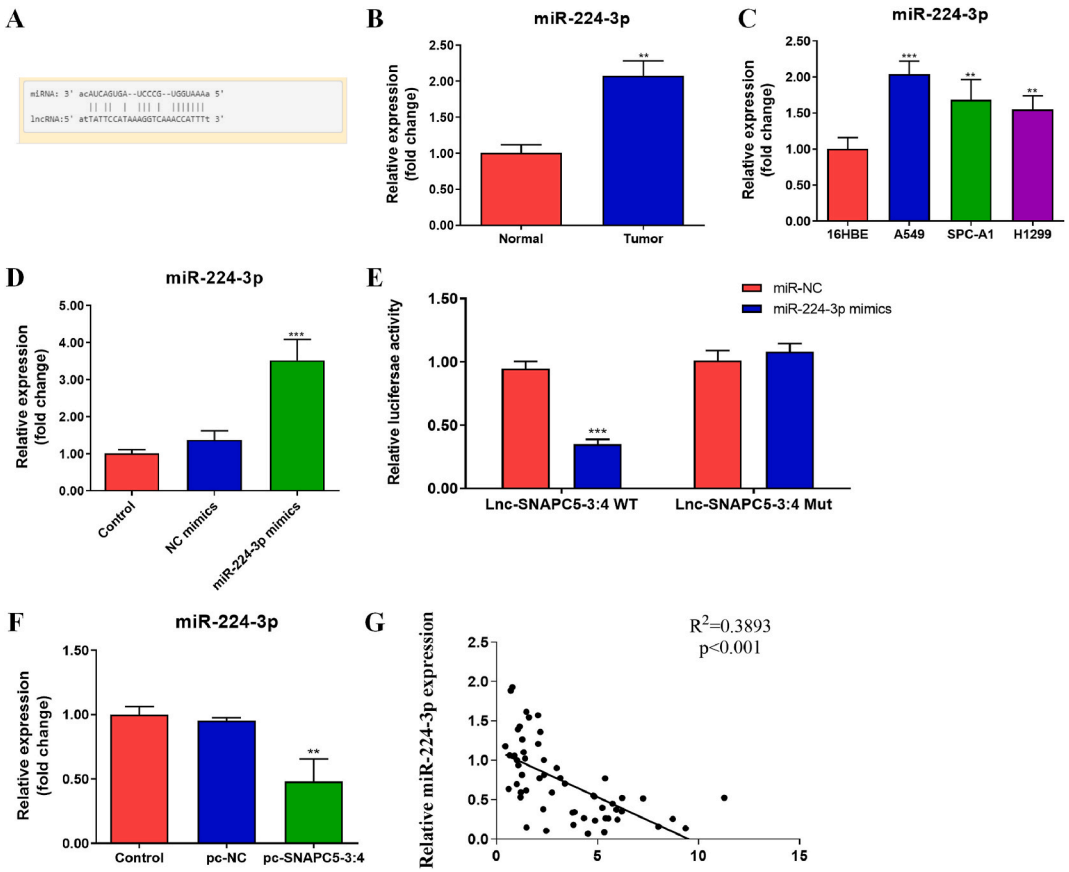

Fig. 3. The regulation of lnc-SNAPC5-3:4 and miR-224-3p expression A. The binding sites of lnc-SNAPC5-3:4 and miR-224-3p. B. Expression of miR-224-3p in non-small cell lung cancer (NSCLC) and paracancerous tissues. C. Expression of lnc-SNAPC5-3:4 in NSCLC cell lines. D. Efficiency of miR-224-3p overexpression in A549 cells. E. Dual-luciferase assay was used to detect the binding of lnc SNAPC5-3:4 to miR-224-3p. F. Effect of SNAPC5-3:4 overexpression on miR-224-3p expression. G. Spearman's correlation analysis of miR-224-3p expression correlating with SNAPC5-3:4. Data are shown as mean ± SD, **P < 0.01, ***P < 0.001.

was upregulated in tumor tissues compared with that in adjacent tissues (Fig. 3B). Furthermore, miR-224-3p expression was substantially higher in the three tumor cell lines than in 16HBE cells, with A549 cells exhibiting a relatively higher expression (Fig. 3C). Efficiency of miR-224-3p overexpression in A549 cells was detected by RT-PCR assay (Fig. 3D).

To confirm this predicted interaction, we performed dual-luciferase assays, which demonstrated that lnc-SNAPC5-3:4 and miR-224-3p indeed bound at the predicted binding site (Fig. 3E). Moreover, overexpression of lnc-SNAPC5-3:4 in A549 cells resulted in a significant downregulation of miR-224-3p expression (Fig. 3F). Finally, Spearman correlation analysis demonstrated a negative correlation between miR-224-3p and lnc-SNAPC5-3:4 expression in both tumor and adjacent tissues (Fig. 3G).

3.4. The lnc-SNAPC5-3:4 impedes proliferation and facilitates apoptosis of NSCLC cells via sponge adsorption of miR-224-3p

To verify whether lnc-SNAPC5-3:4 hinders the malignant progression of lung cancer cells by specifically binding to miR-224-3p, we introduced additional miR-224-3p into A549 cells overexpressing lnc-SNAPC5-3:4 (Fig. 4A). We observed that the activity and proliferation of A549 with lnc-SNAPC5-3:4 overexpression were significantly suppressed. However, this inhibition was nearly abolished by the introduction of miR-224-3p (Fig. 4B and C). Remarkably, miR-224-3p also reversed the promoting effect of lnc-SNAPC5-3:4 on A549 cell apoptosis, as evidenced by a decrease in the expression of Bax and Caspase 3 with increasing levels of miR-224-3p (Fig. 4D and E).

3.5. The lnc-SNAPC5-3:4 inhibits tumor growth in vivo via sponge adsorption of miR-224-3p

We further investigated the impact of targeted regulation of lnc-SNAPC5-3:4 and miR-224-3p on tumor cell growth *in vivo* by subcutaneously injecting differently treated A549 cells and control cells into nude mice. Remarkably, in nude mice, the overexpression of both lnc-SNAPC5-3:4 and miR-224-3p maintained considerable levels of expression (Fig. 5A and B). Notably, based on the analysis of tumor images, tumors in the lnc-SNAPC5-3:4 overexpression group exhibited the smallest volume and weight; however, the addition

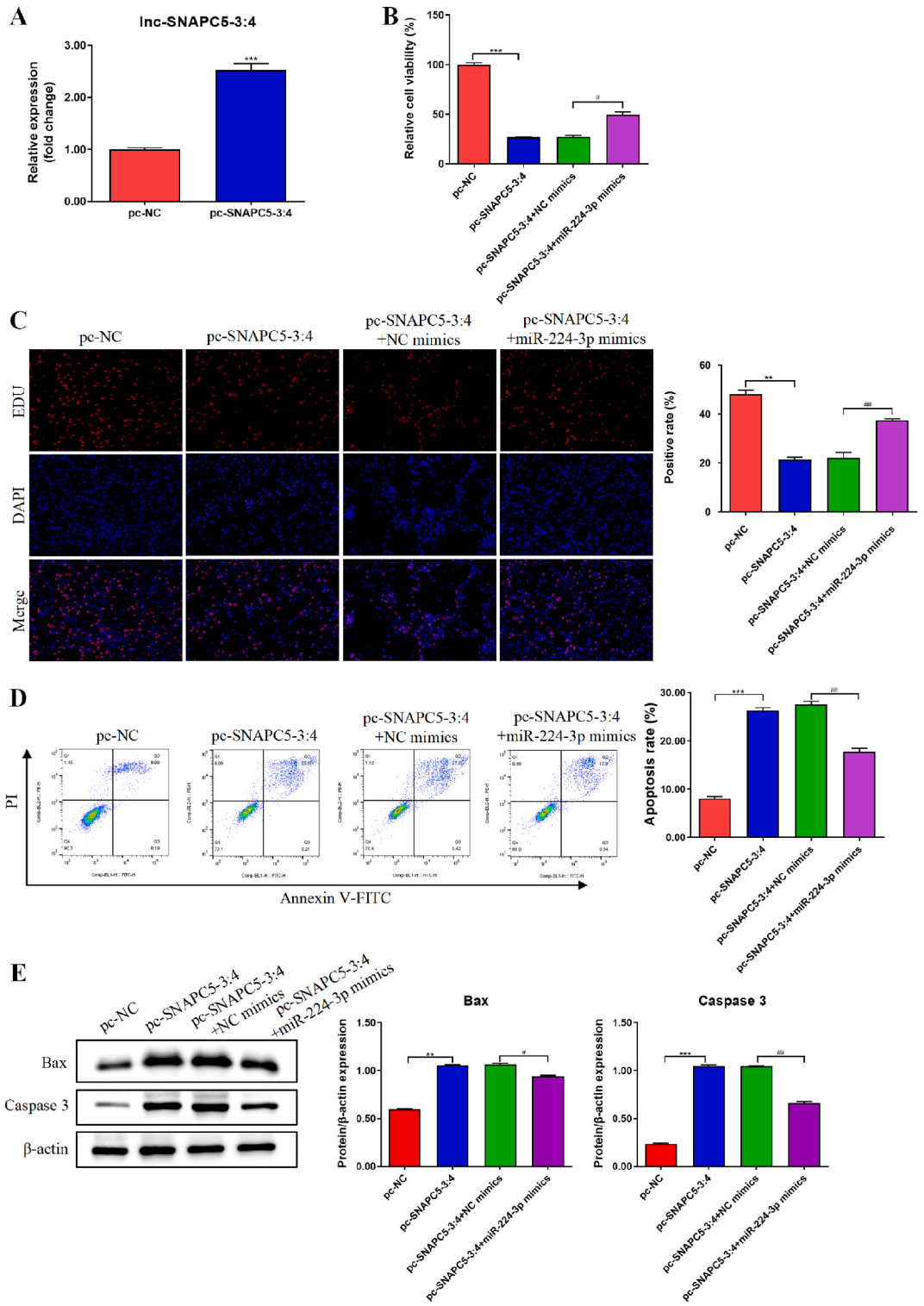

Fig. 4. The lnc-SNAPC5-3:4 inhibits proliferation and promotes apoptosis of non-small cell lung cancer (NSCLC) cells by sponge adsorption of miR-224-3p. A. Efficiency of lnc-SNAPC5-3:4 overexpression in A549 cells. B. The activity of A549 cells was determined using a Cell Counting Kit-8 (CCK-8) assay. C. The proliferation of A549 cells was detected using the 5-ethynyl-2′-deoxyuridine (EdU) assay. D. The apoptosis of A549 cells was detected using fluorescence-activated cell sorting (FACS). E. The expression levels of Bax and Caspase3 in A549 cells were determined using western blotting. Data are shown as mean ± SD, *P < 0.05, **P < 0.01, ***P < 0.001.

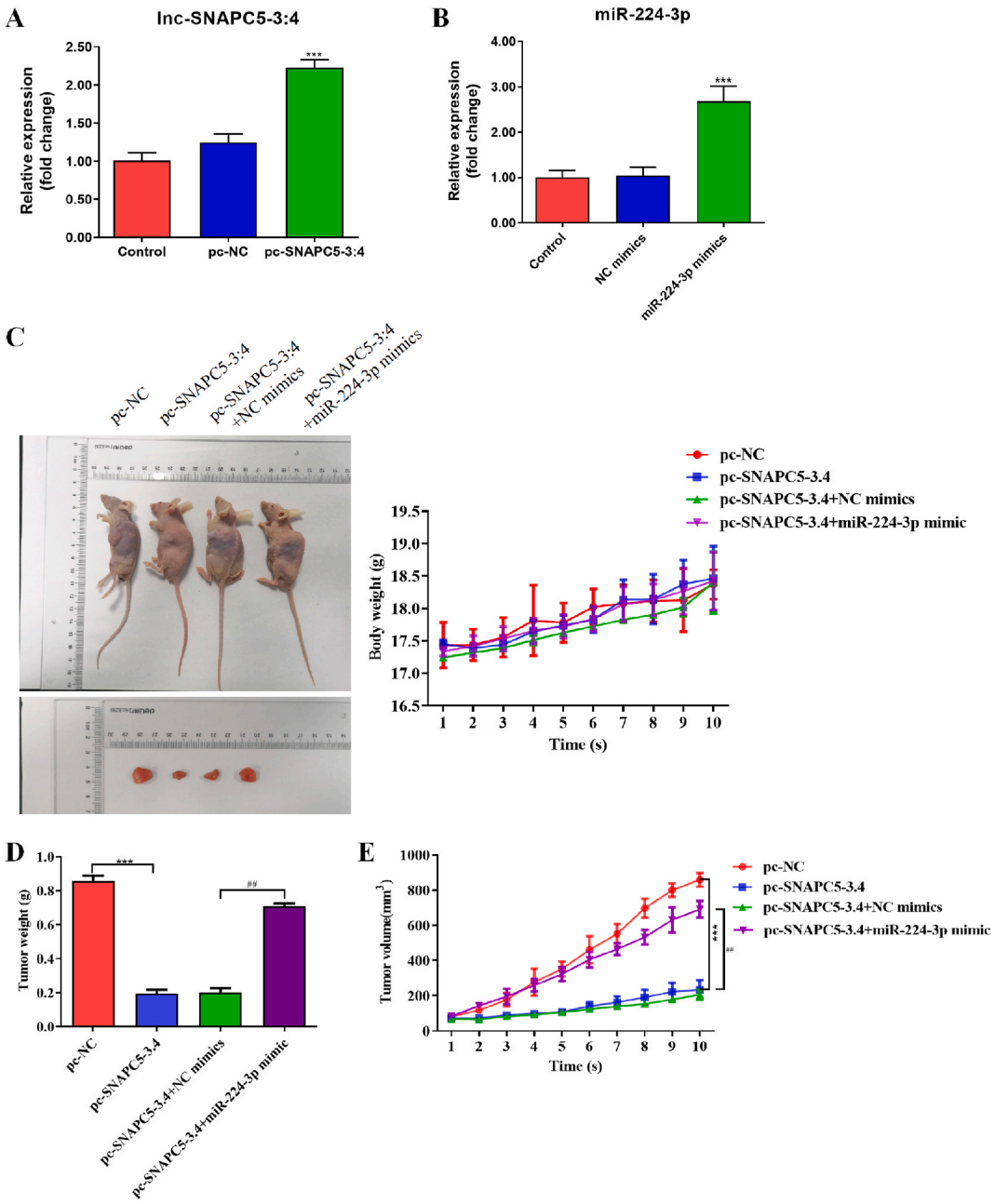

Fig. 5. The lnc-SNAPC5-3:4 inhibits the growth of non-small cell lung cancer (NSCLC) tumors by sponge adsorption of miR-224-3p *in vivo*. A. Expression of lnc-SNAPC5-3:4 in tumor tissues of nude mice. B. Expression of miR-224-3p in tumor tissues of nude mice. C. Images of nude mice and tumors. D. Tumor weight. E. Tumor growth curve. ***P < 0.001.

of miR-224-3p resulted in an incremental increase in tumor volume and weight (Fig. 5C–E). These findings highlight the precise *in vivo* inhibitory function of lnc-SNAPC5-3:4 on tumor growth through the specific suppression of miR-224-3p.

In this study, we used immunohistochemistry to assess the proliferation-related protein Ki67 in the tumor tissues from each experimental group. Consistent with tumor growth, we noted a reduction in Ki67 expression in the pc-SNAPC5-3:4 group, whereas Ki67 expression increased in the pc-SNAPC5-3:4 + miR-224-3p mimic group (Fig. 6A). Additionally, TUNEL staining was used to evaluate the apoptotic levels in the respective tumor tissues. Apoptosis was enhanced in the pc-SNAPC5-3:4 group and decreased in the pc-SNAPC5-3:4 + miR-224-3p mimic group (Fig. 6B). Furthermore, the expression of Bax and Caspase3 was upregulated in the pc-SNAPC5-3:4 group but downregulated in the pc-SNAPC5-3:4 + miR-224-3p mimic group (Fig. 6C). This finding is consistent with our *in vitro* experiments, implying that lnc-SNAPC5-3:4 exhibits inhibitory effects on A549 proliferation and facilitates apoptosis, primarily by sequestering miR-224-3p.

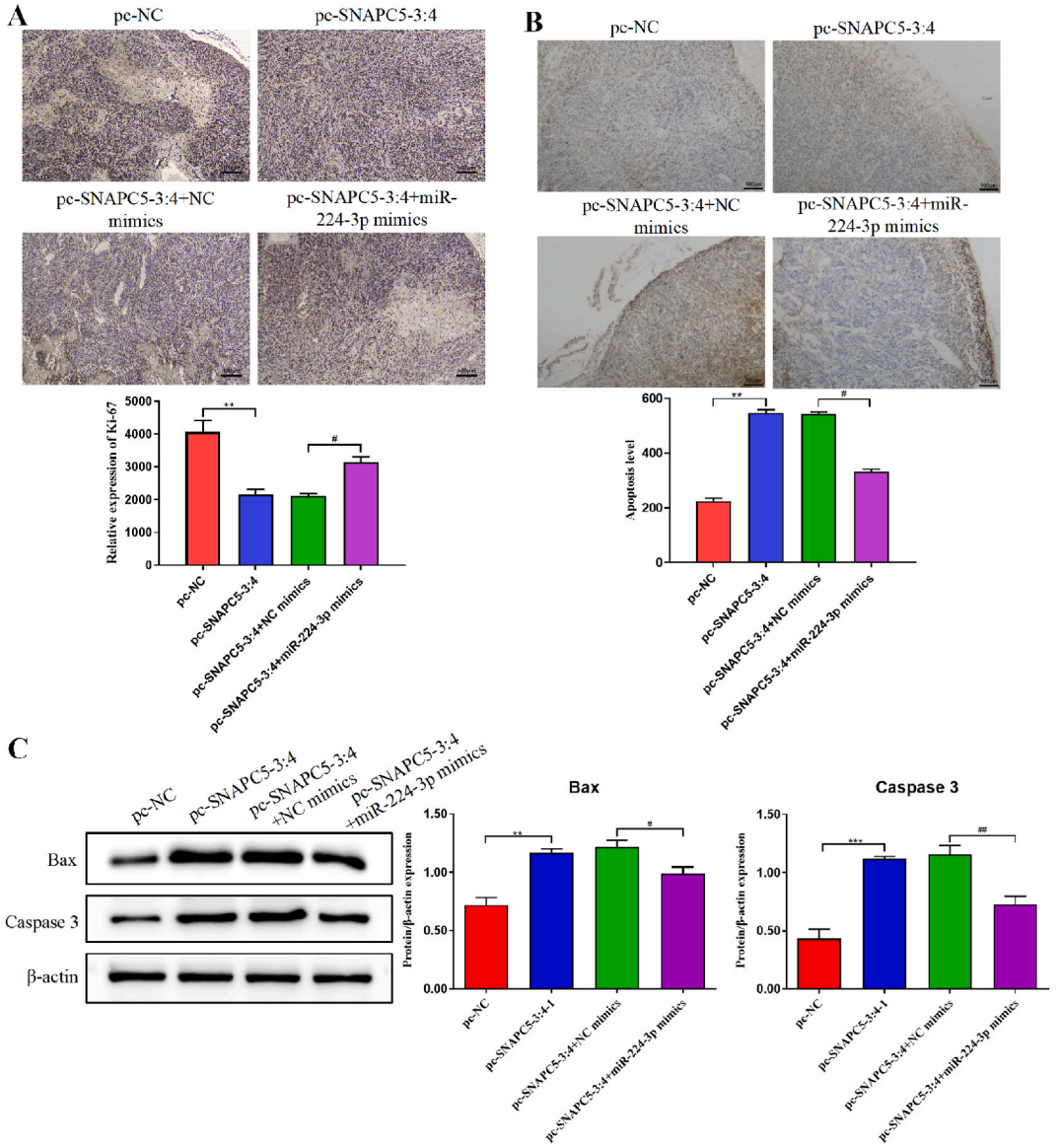

Fig. 6. Signaling pathway changes in tumors. A. The expression level of the proliferation-related protein antigen Kiel 67 (Ki67) was detected using immunohistochemistry (IHC). B. Apoptosis was detected using terminal deoxynucleotidyl transferase dUTP nick end labeling (TUNEL) staining. C. The expression levels of Bax and Caspase3 in the tumors were determined using western blotting. Data are shown as mean ± SD, *P < 0.05, **P < 0.01.

4. Discussion

Lung cancer has been ranked as the leading cause of cancer-related death in humans [14]. A large number of studies have shown that the abnormal expression of lncRNA and miRNA is highly correlated with the development of lung cancer [14]. For example, SOX21-AS1 levels were significantly increased while miR-24-3p levels were significantly decreased in lung cancer tissues and cells. SOX21-AS1 increased the proliferation, migration, and invasion of A549 and HCC827 cells by targeting miR-24-3p [6]. In addition, a previous study reported that the expression level of lnc-SNAPC5-3:4 in plasma exosomes of NSCLC patients was significantly down-regulated [7]. miR-224-3p was highly expressed in lung cancer cells A549 and Calu-3 [14]. Similar to previous studies, we found that lnc-SNAPC5-3:4 was significantly down-regulated in clinical tissue samples of NSCLC patients and lung cancer cells, which was also verified at the *in vivo* animal level, while the expression level of miR-224-3p was opposite to lnc-SNAPC5-3:4.

A large number of studies have shown that lncRNA is usually associated with the occurrence and progress of tumors, some of these disorders in various human cancers, lncRNA can serve as a promising NSCLC prognostic marker [16]. For instance, lncRNA HOTAIR showed a significant increase in NSCLC tissues compared with that in control paracancerous tissues, exhibiting a specificity of 86.9 %

and sensitivity of 52.3 % [17]. Additionally, serum exosomal lncRNA SNHG15 was markedly elevated in patients with NSCLC compared with that in patients with benign lung disease and normal controls [18]. LNC CRYBG3 overexpression caused M-phase arrest and promoted lung cancer cell death, as well as inhibited cell proliferation *in vitro* and *in vivo* [16]. Studies have shown that plasma exosomal lnc-SNAPC5-3:4 is significantly up-regulated when anlotinib treatment is effective but down-regulated when anlotinib treatment fails [7]. However, the molecular mechanism of lnc-SNAPC5-3:4 in NSCLC is still unknown. In this study, we have confirmed the established expression lnc-SNAPC5-3:4 inhibits NSCLC cell proliferation and promotes cell apoptosis. Moreover, lnc-SNAPC5-3:4 overexpression impaired NSCLC tumorigenesis *in vivo*.

Additionally, lncRNAs indirectly regulate target genes through miRNA sponge adsorption, an important regulatory mechanism in NSCLC, thereby providing a new way to study the pathogenesis and development of this disease [19]. Many interactions between lncRNAs and miRNAs have been identified [20]. For instance, the lncRNA XIST is abnormally overexpressed in NSCLC tissues and cell lines, and miR-335 is a downstream target of lncRNA-XIST. Elevated expression of lncRNA XIST enhances superoxide dismutase 2 (SOD2) levels by sequestering miR-335 through sponge adsorption. Silencing of lncRNA XIST triggers pyroptosis via the miR-335/SOD2 signaling pathway, thereby inhibiting the progression of NSCLC cells [21]. Consistently, we showed that miR-224-3p serves as a tumor suppressor in NSCLC. The upregulation of miR-224-3p prevented cell proliferation and increased the proportion of apoptotic cells, whilst lnc-SNAPC5-3:4 overexpression partially reversed these effects, indicating that the function of miR-224-3p is regulated by lnc-SNAPC5-3:4. Collectively, the lnc-SNAPC5-3:4/miR-224-3p axis plays a pivotal role in NSCLC progression.

Taken together, our results confirm that lnc-SNAPC5-3:4 inhibits the malignant progression of lung cancer by targeting the negative regulation of miR-224-3p, and these findings provide new insights into the regulatory function of lnc-SNAPC5-3:4 and miR-224-3p in NSCLC.

Availability of data and materials

All the data used in this study is available from the corresponding authors upon reasonable request.

Funding

This work was supported by the Xuzhou Medical University Affiliated Hospital Science and Technology Development Fund (XYFM2021047).

Animal ethics

All animal experiments were approved by the Animal Care and Use Committee of Bestcell Model Biological Center (NO.2023-07-24A). The methods were carried out following the approved guidelines.

CRediT authorship contribution statement

Chenxi Hu: Writing – original draft, Investigation. **Shuo Wu:** Project administration, Methodology, Formal analysis, Data curation. **Wen Sun:** Software, Resources, Project administration. **Jiawen Li:** Visualization, Supervision, Software. **Kaiyuan Hui:** Writing – original draft, Investigation, Data curation, Conceptualization. **Xiaodong Jiang:** Writing – review & editing, Conceptualization.

Declaration of competing interest

The authors declare that they have no known competing financial interests or personal relationships that could have appeared to influence the work reported in this paper.

Appendix A. Supplementary data

Supplementary data to this article can be found online at https://doi.org/10.1016/j.heliyon.2024.e24668.

References

[1] R.L. Siegel, K.D. Miller, N.S. Wagle, A. Jemal, Cancer statistics, 2023, CA A Cancer J. Clin. 73 (2023) 17–48.
[2] H. Guo, Z. Chang, J. Wu, W. Li, Air pollution and lung cancer incidence in China: who are faced with a greater effect? Environ. Int. 132 (2019) 105077.
[3] Q. Hu, H. Ma, H. Chen, Z. Zhang, Q. Xue, LncRNA in tumorigenesis of non-small-cell lung cancer: from bench to bedside, Cell Death Dis. 8 (2022) 359.
[4] Y.T. Tan, J.F. Lin, T. Li, J.J. Li, R.H. Xu, H.Q. Ju, LncRNA-mediated posttranslational modifications and reprogramming of energy metabolism in cancer, Cancer Commun. 41 (2021) 109–120.
[5] P.F. Jiao, P.J. Tang, D. Chu, Y.M. Li, W.H. Xu, G.F. Ren, Long non-coding RNA THOR depletion inhibits human non-small cell lung cancer cell growth, Front. Oncol. 11 (2021) 756148.
[6] F. Wang, T. Gu, Y. Chen, Y. Chen, D. Xiong, Y. Zhu, Long non-coding RNA SOX21-AS1 modulates lung cancer progress upon microRNA miR-24-3p/PIM2 axis, Bioengineered 12 (2021) 6724–6737.

[7] C. Liu, C. Hu, T. Chen, Y. Jiang, X. Zhang, H. Liu, Y. Wang, Z. Li, K. Hui, X. Jiang, The role of plasma exosomal lnc-SNAPC5-3:4 in monitoring the efficacy of anlotinib in the treatment of advanced non-small cell lung cancer, J. Cancer Res. Clin. Oncol. 148 (2022) 2867–2879.
[8] P. Zhao, Q. Zhao, C. Chen, S. Lu, L. Jin, miR-4757-3p inhibited the migration and invasion of lung cancer cell via targeting Wnt signaling pathway, JAMA Oncol. 2023 (2023) 6544042.
[9] T.Y. Chao, T. Kordass, W. Osen, S.B. Eichmuller, SOX9 is a target of miR-134-3p and miR-224-3p in breast cancer cell lines, Mol. Cell. Biochem. 478 (2023) 305–315.
[10] W. Fang, S. Shu, L. Yongmei, Z. Endong, Y. Lirong, S. Bei, miR-224-3p inhibits autophagy in cervical cancer cells by targeting FIP200, Sci. Rep. 6 (2016) 33229.
[11] Y. Jia, C. Tian, H. Wang, F. Yu, W. Lv, Y. Duan, Z. Cheng, X. Wang, Y. Wang, T. Liu, J. Wang, L. Liu, Long non-coding RNA NORAD/miR-224-3p/MTDH axis contributes to CDDP resistance of esophageal squamous cell carcinoma by promoting nuclear accumulation of beta-catenin, Mol. Cancer 20 (2021) 162.
[12] R. Xu, F. Feng, X. Yu, Z. Liu, L. Lao, LncRNA SNHG4 promotes tumour growth by sponging miR-224-3p and predicts poor survival and recurrence in human osteosarcoma, Cell Prolif. 51 (2018) e12515.
[13] G. Wang, L. Liu, J. Zhang, C. Huang, Y. Chen, W. Bai, Y. Wang, K. Zhao, S. Li, LncRNA HCG11 suppresses cell proliferation and promotes apoptosis via sponging miR-224-3p in non-small-cell lung cancer cells, OncoTargets Ther. 13 (2020) 6553–6563.
[14] F. Yan, W. Zhao, X. Xu, C. Li, X. Li, S. Liu, L. Shi, Y. Wu, LncRNA DHRS4-AS1 inhibits the stemness of NSCLC cells by sponging miR-224-3p and upregulating TP53 and TET1, Front. Cell Dev. Biol. 8 (2020) 585251.
[15] G. Wang, J. Han, L. Zhuang, S. Li, Q. Gong, Y. Chen, Serum starvation induces cell death in NSCLC via miR-224, OncoTargets Ther. 12 (2019) 3953–3962.
[16] W. Mao, Z. Guo, Y. Dai, J. Nie, B. Li, H. Pei, G. Zhou, LNC CRYBG3 inhibits tumor growth by inducing M phase arrest, J. Cancer 10 (2019) 2764–2770.
[17] X. Yao, T. Wang, M.Y. Sun, Y. Yuming, D. Guixin, J. Liu, Diagnostic value of lncRNA HOTAIR as a biomarker for detecting and staging of non-small cell lung cancer, Biomarkers 27 (2022) 526–533.
[18] P. Han, J. Zhao, L. Gao, Increased serum exosomal long non-coding RNA SNHG15 expression predicts poor prognosis in non-small cell lung cancer, J. Clin. Lab. Anal. 35 (2021) e23979.
[19] S. Ghafouri-Fard, H. Shoorei, W. Branicki, M. Taheri, Non-coding RNA profile in lung cancer, Exp. Mol. Pathol. 114 (2020) 104411.
[20] M. Ratti, A. Lampis, M. Ghidini, M. Salati, M.B. Mirchev, N. Valeri, J.C. Hahne, MicroRNAs (miRNAs) and long non-coding RNAs (lncRNAs) as new tools for cancer therapy: first steps from bench to bedside, Targeted Oncol. 15 (2020) 261–278.
[21] J. Liu, L. Yao, M. Zhang, J. Jiang, M. Yang, Y. Wang, Downregulation of LncRNA-XIST inhibited development of non-small cell lung cancer by activating miR-335/SOD2/ROS signal pathway mediated pyroptotic cell death, Aging (Albany NY) 11 (2019) 7830–7846.